

MACHINING MODEL OF Ti-6Al-4V TITANIUM ALLOY USING FEM SIMULATION

Hadzley, M.M.A., Raja Izamshah, R.A., Amran, M.M.A.

Department of Manufacturing Process,
Faculty of Manufacturing Engineering,
Universiti Teknikal Malaysia Melaka,
Hang Tuah Jaya, 76100
Durian Tunggal, Melaka, Malaysia

Email: hadzley@utem.edu.my

ABSTRACT: This paper presents a machining model of Ti-6Al-4V titanium alloy using finite element method (FEM) simulation. The constitutive Johnson–Cook material flow stress was employed to predict material plasticity, chip morphology, cutting forces and stress distribution. Comparative analysis for both simulation and experimental data were carried out. The simulated results show that workpiece material flow around the cutting edge of the tool and deposited themselves to form a continuous curl chip formation. The stress distribution generated in the shearing plane during steady state conditions and the residual stress is formed beneath the machined surface. The cutting forces were essentially constant across the range of cutting speeds. This agreed with the trend from the experimental trials.

KEYWORDS: Machining, Ti-6Al-4V alloy, FEM.

1.0 INTRODUCTION

Since their introduction in the early 1950s, Ti-6Al-4V alloys have become the backbone materials of choice for aerospace, marine, medical and other major industrial applications. The combination of high strength-to-weight ratio, excellent mechanical properties and corrosion resistance have led to titanium alloys being used in a wide and diversified range of successful applications (Ezugwu, E. O., Bonney, J. and Da Silva, R. B., 2007) However, this material is known to be difficult to machine due to its low thermal conductivity which gives rise to high temperatures at the tool–chip and tool-workpiece interfaces. Therefore, the cutting process of Ti-6Al-4V is associated with complex physical phenomenon which is difficult to comprehend by direct experimental alone.

Over the past two decades, finite element method (FEM) has been used extensively in the investigation of machining processes. Some of the commercial software that can simulate machining process are Nike2D, Abaqus, Marc, Deform, Forge, Algor, Fluent, Advantedge and Ls-Dyna (Soo, S.L. and Aspinwall, D.K., 2007). Early simulations of machining processes were carried out by Usui and Shirakashi (Usui, E. and Shirakashi, T., 1982) by analyzing steady-state orthogonal cutting. Carroll and Strenkowski (Carroll, J.T. and Strenkowski, C., 1998), attempted chip formation and separation from the workpiece. Hua and Shivpuri (Hua, J. and Shivpuri, R., 2004), simulated chip formation of machining based on deformation energy-based criterion (Umbrello, D., 2008) focussed on damage criterion and friction to simulate chip morphology during machining. To deal with large element distortion, (Rui, L. and Shih, A. J., 2006), developed 3D model to simulate chip formation during machining. (Calamaz *et.al* 2008), Calamaz modified the Johnson-Cook constitutive model to simulate serrated chip formation. Many studies have described the stability and the simulation of the machining process for hardened metal and high strength alloy. However, few works consider the machining simulation of Ti-6Al-4V alloy.

In this study, FEM machining simulations of Ti-6Al-4V alloy is carried out using commercially available software Ls-Dyna 4.21. The purpose of the study is to understand the underlying mechanism when machining Ti-6Al-4V alloy. A simulation model of machining process have been developed based on the Lagrangian formulation with Johnson-Cook plasticity model. Experimental chip formation, together with cutting force data were compared with the predicted output from the model. Correct simulation of the cutting process enables good predictions in terms of chip formation, strain and stress distribution at the cutting interfaces. This will contribute to significant cost reduction for machining process optimisation which at the moment is still carried out experimentally.

2.0 METHODOLOGY

2.1 Finite element model

Figure 1 shows the FEM model for the cutting process. Lsprepost 2.1 was used to prepare finite element mesh. The workpiece material was built from 8012 nodes and 3000 element while the cutting tool was built from 2134 nodes and 768 elements. Boundary conditions were applied on the bottom and right side nodes of the workpiece and the tool was

constrained against vertical displacement and rotation. The total time of simulated machining process was 2.0ms with cutting speeds varied from 110 m/min to 130 m/min and feed rate constant at 0.15 mm/rev. For simplicity, a cutting tool was modelled as rigid and the coefficient of friction between cutting tool and workpiece material was assumed to be 0.3 based on the coulomb friction law.

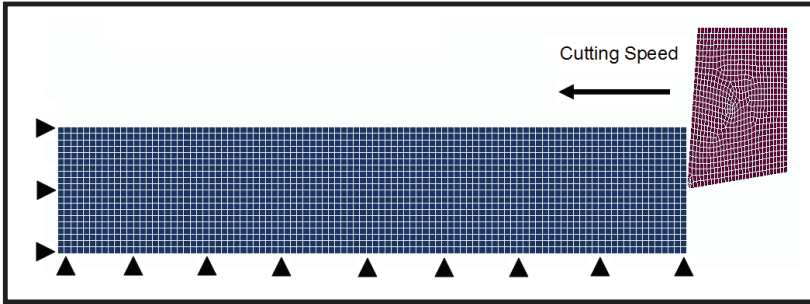


Figure1 FEM model for the cutting process

2.2 Material Properties

To describe the material response, the constitutive model proposed by Johnson-Cook was utilized in this study. Johnson-Cook material model is expressed by

$$\sigma = \left[A + B \epsilon^n \right] \left[1 + C \ln \frac{\epsilon'}{\epsilon'_o} \right] \left[1 - \frac{T - T_o}{T_{melt} - T_o} \right]^m \dots\dots\dots(3.1)$$

where σ is the flow stress, ϵ is the plastic strain, ϵ' is the strain rate, ϵ'_o is the reference plastic strain, T is the workpiece temperature, T_{melt} is the melting temperature of the workpiece material and T_o is the room temperature. The constant coefficient A is the yield strength, B is the hardening modulus, C is the strain rate sensitivity coefficient, n is the hardening coefficient and m is the thermal softening coefficient. All parameters used in this study were determined by Lee and Lin (Lee, W.S. and Lin, C.F., 1998), as shown in Table 1.

Table 1 Overview of the material properties used in the simulations

A(MPa)	B(MPa)	C	n	m	$\dot{\epsilon}_0(s^{-1})$	T_0 (K)	$T_{melt}(K)$	Failure strain
782.7	498.4	0.028	0.28	1	$1e-5 s^{-1}$	300	1800	0.3

2.3 Experimental Setup and Verification

The results of FEM models were verified with the machining trials of commercially available Ti-6Al-4V alloy. Setup for the machining tests is shown in Figure 2(a). The component forces were measured using a dynamometer with oscilloscope as shown in Figure 2(b). The following cutting conditions were employed in this investigation:

Cutting Speed (m/min): 110, 120 and 130
 Feed rate (mm/rev): 0.15

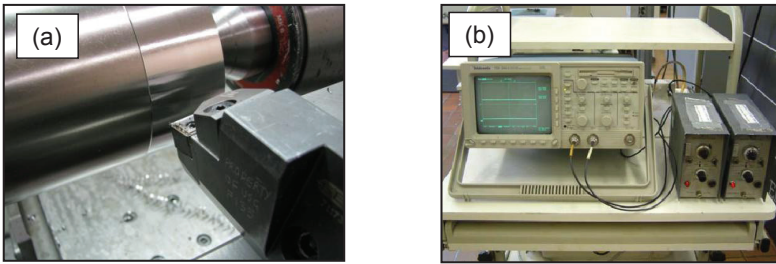


Figure 2 Experimental setup for machining verification. (a) Machining setup (b) Dynamometer complete with oscilloscope for recording cutting forces.

3.0 RESULTS AND DISCUSSIONS

3.1 Simulation Results

The result of the initial chip formation when modelling of machining Ti-6Al-4V is shown in Figure 3. It is clearly shown that heavy plastic deformation was visible around the region where the cutting tool penetrated into the workpiece. This region is characterized by the relatively large mesh distortion where meshes that sufficiently strained around 0.3 were automatically deleted to facilitate chip separation. It can be seen from Figure 3 that the deformation of the chip distorted heavily at the initial contact point (Figure 3a), then increasing sharply along tool rake face (Figure 3b) and dropping quickly to form a continuous chip curl (Figure 3c).

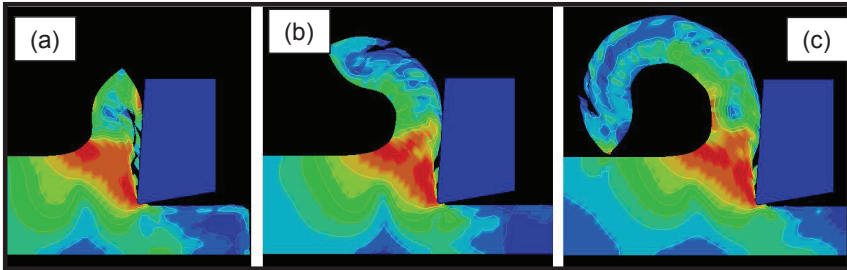


Figure 3 Chip formation during machining with 110 m/min cutting speed at times of:(a) 0.0005 s (b) 0.001s (c) 0.002 s

Figure 4 shows the comparison between experimental and FEM results for the chip curl when machining T-6Al-4V alloy at 110 m/min speed. Qualitatively, the morphology of the chip curl obtained from experiment (Figure 4(a)) and FEM model (Figure 4(b)) is generally similar. The chip flow direction is also similar for both the simulated and experimental data. However, the finite element method tends to under-predict the diameter of the experimental chip curl by about 33-41% as shown in Table 4. One possible cause according to Rui and Shih (Rui, L. and Shih, A. J., 2006), is the contact condition of the chip with the tool and workpiece during machining. In actual machining, contact conditions such as chamfer and tool nose radius significantly affect the contact length and width of the chips in lateral and axial directions while in finite element modelling, especially in 2D, contact between the tool and the workpiece was simplified from the friction, flow stress and cutting parameters.

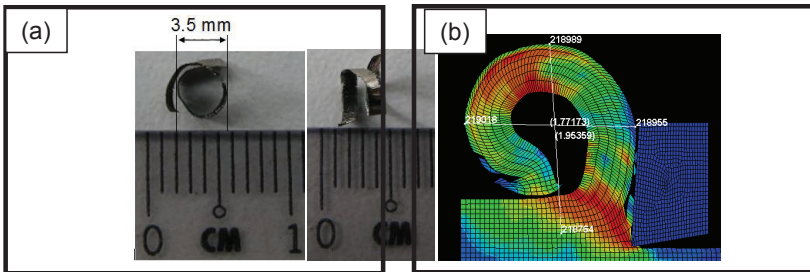


Figure 4 Comparison of chip curl when machining at a speed of 110 m/min (a) experimental (b) simulation

Table 4 Comparison of chips diameter for experiments and simulation

Cutting Speeds	110 m/min	120 m/min	130 m/min
Experiment	2.5-3.5mm	2.8-3.7 mm	2.9-3.9 mm
Simulation	1.72-2.18 mm	1.83-2.23 mm	1.85-2.28 mm
Difference	33-37 %	35-39 %	36-41 %

3.2 Cutting Forces

Figure 5 shows the plots of recorded cutting forces from the experimental tests and those from the simulations. The value of cutting forces is fluctuated due to the instability of chip-tool contact resulting from tool geometry and elasticity of work material as shown in Figure 7. The cutting forces recorded experimentally ranged from 200-208 N whereas, the simulated cutting forces ranged from 180-184 N as shown in Figure 6. On average, the simulated data were generally lower than the experimental data by 11 %. The difference between experimental and simulation results appear to be reasonable since the FEM model is developed with some simplifications and constant assumptions have been introduced such as friction coefficient and material constitutive model (Yung-Chang, Y., *et.al.*, 2004)

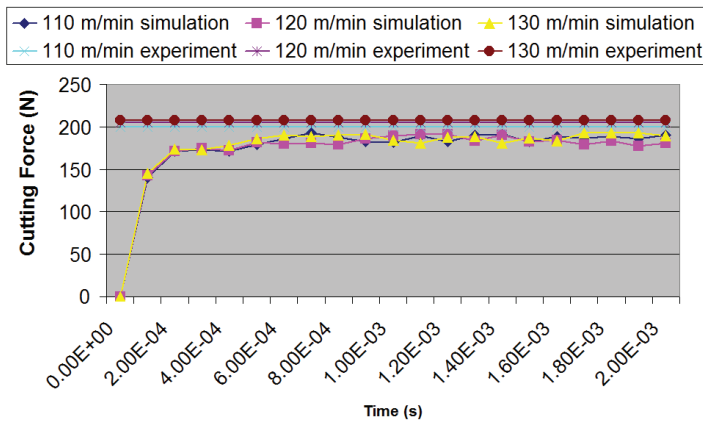


Figure 5 Cutting force distribution in 2 ms.

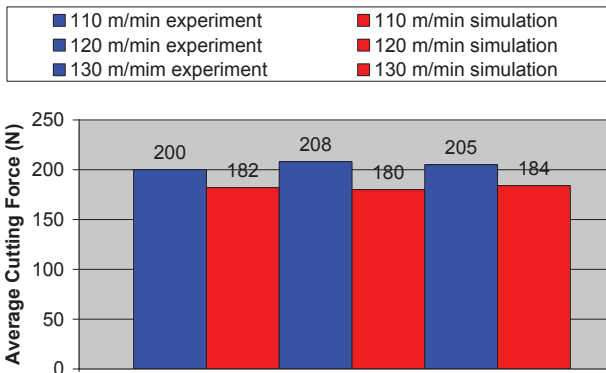


Figure 6 Comparison between experimental and simulated cutting forces

3.3 Stress Distribution

Figure 7 shows the distribution of stress in the work material after 0.005 s machining for 110 m/min. From the stress field contour plots, one can observe that plastic deformation occurs in three regions: the primary deformation zone which stretches from the tool tip to the free surface of the workpiece; the secondary deformation zone which occurs along the rake face of the cutting tool and the tertiary deformation zone which occurs under the tool–chip interface. The primary deformation zone represent the adiabatic shear plane in cutting zone where large stresses are imparted to the chip. In particular, it is noted that chip materials just ahead of the tool tip experience a high level of stress against the tool, which reflect the abrasive action of the chip upon the tool tip (Lee W. S. and Lin C. F., 1998). The secondary deformation zone illustrates sliding motion of the chip on the rake face of the tool. Contact instabilities appeared in this zone as a result of complex interaction between friction, temperature generation and thermal softening of the work material (Lee, W. S. and Lin, C. F., 1998). This situation induces fluctuation in cutting force and represents the action of adhesive wear in the tool–chip interface (Lee, W. S. and Lin, C. F., 1998). The tertiary deformation zone illustrates stress in the workpiece occurred just below and behind the tool tip. The stresses still remain in the surface of the machined workpiece even when the cutting tool is far away from the shearing point. This stress is expected to have a strong influence on the formation of residual stresses in the workpiece. Excessive residual stress affects the surface integrity causing surface alteration, microhardnes changes and decreased fatigue life of the machined components (Ezugwu, E. O., Bonney, J. and Da Silva, R. B., 2007).

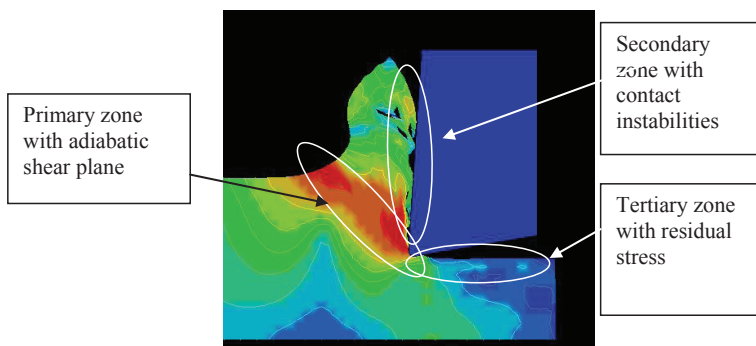


Figure7 Stress contours from the simulation after 0.005 s for 110 m/min cutting speed

4.0 CONCLUSIONS

This paper presents a modelling of machining of Ti-6Al-4V titanium alloy FEM simulation. The Johnson–Cook’s constitutive equation was implemented and the results were compared with experimental data. Results obtained indicate that a reasonable prediction of chip morphology and cutting forces for both experimental and simulation. The machining simulation illustrates the distribution of stress in the primary, secondary and tertiary deformation zones which represent the interaction of cutting tool and work material during machining. The FE strategy proposed in this paper generally can be employed to study the machining process of Ti-6Al-4V alloy and to predict the cutting forces and the chip formation with reasonable accuracy.

5.0 REFERENCES

- Ezugwu, E. O., Bonney, J. and Da Silva, R. B., 2007, “Surface Integrity of Finished Turned Ti-6Al-4V Alloy with PCD Tools using Conventional and High Pressure Coolant Supplies”, *International Journal of Machine Tools & Manufacture*, Vol. 47, 2007, pp. 884–891.
- Soo, S.L. and Aspinwall, D.K., 2007, “Developments in Modelling of Metal Cutting Processes, Proc. Mech E, part I. – Design and Applications. Orlando, USA, Vol. 221, 2007, pp.197-211.
- Usui, E. and Shirakashi, T., 1982, “Mechanics of Machining - From Descriptive to Predictive Theory. On the Art of Cutting Metals - 75 Years Later. ASME Publication, Vol. 7, 1982, pp.13-35.
- Carroll, J.T. and Strenkowski, C., 1998, “Finite Element Models Of Orthogonal Cutting With Application To Single Point Diamond Turning’, *International Journal Of Mechanical Science*, Vol. 30, No. 12, 1998, pp. 899-920.
- Hua, J. and Shivpuri, R., 2004, “Prediction of Chip Morphology and Segmentation During the Machining of Titanium Alloys, *Journal of Materials Processing Technology*, Vol. 150, 1-2, 2004, pp. 124-133.
- Umbrello, D., 2008, “Finite Element Simulation of Conventional and High Speed Machining of Ti6Al4V Alloy, *Journal of Materials Processing Technology*, Volume 196, Vol. 1-3, 2008, pp. 79-87.
- Rui, L. and Shih, A. J., 2006, “Finite Element Modeling of 3D Turning of Titanium”, *International Journal of Advanced Manufacturing Technology*, Vol. 29, 2006, pp. 253–261.
- Calamaz, M., Dominique, C. and Franck, G. 2008, “A New Material Model for 2D Numerical Simulation of Serrated Chip Formation when Machining Titanium Alloy Ti-6Al-4V”, *International Journal of Machine Tools and Manufacture*, Vol. 48, Issues 3-4, 2008, pp. 275-288.

- Ls-dyna., 2007, User's Keyword Manual, Volume 1, Version 971, LTSC, May 2007.
- Trent, E. M., 1991, Metal Cutting, Fourth Edition, Butterworth-Heinemann Ltd., 1991.
- Yung-Chang, Y., Anurag, J. and Taylan A., 2004, A Finite Element Analysis of Orthogonal Machining using Different Tool Edge Geometries, Journal of Materials Processing Technology, Vol. 146, 2004, pp. 72–81.
- Lee W. S. and Lin C. F., 1998, "Plastic Deformation and Fracture Behaviour of Ti-6Al-4V Alloy, Loaded with High Strain Rate under Various Temperatures", Materials Science and Engineering A, Vol. 241, 1998, pp. 48–59.

